Robotica (2022), **40**, pp. 1309–1325
doi:10.1017/S0263574721001120

CAMBRIDGE
UNIVERSITY PRESS

RESEARCH ARTICLE

Robust adaptive controller–observer scheme for robot manipulators: a Bernstein–Stancu approach

Alireza Izadbakhsh[1,*] and Nazila Nikdel[2]

[1]Department of Electrical Engineering, Garmsar Branch, Islamic Azad University, Garmsar, Iran and [2]Faculty of Electrical and Computer Engineering, Urmia University, Urmia, Iran
*Corresponding author. E-mail: izadbakhsh_alireza@hotmail.com

Received: 25 March 2021; **Revised:** 19 June 2021; **Accepted:** 20 July 2021; **First published online:** 28 September 2021

Keywords: function approximation techniques; Bernstein–Stancu operator; controller–observer structure; adaptive control

Abstract

This article introduces a robust adaptive controller–observer structure for robotic manipulators such that the need for joints speed measurement is removed. Besides, it is presumed that the system model has uncertainties and is subject to disturbances, and the proposed method must eliminate the impact of these factors on the system response. According to this, for the first time in the robotics field, a model-free scheme is developed based on the Bernstein–Stancu polynomial. The universal approximation property of the Bernstein–Stancu polynomial enables it to accurately estimate the lumped uncertainty, including unmodeled dynamics and disturbances. Moreover, to increase the efficiency of the controller–observer structure, adaptive rules have been proposed to update polynomial coefficients. The boundedness of all system errors is proven using the Lyapunov theorem. Finally, the proposed robust Adaptive controller–observer is applied on a planer robot, and the results are precisely analyzed. The results of the proposed approach are also compared with two state-of-art powerful approximation methods.

1. Introduction

The rapid advancement of technology has led to the increasing use of robotic systems, especially manipulators. Therefore, the need to provide efficient control methods for them has been raised more than ever. To this end, many recent studies have focused on providing model-based controllers such as the feedback linearization methods for robotic systems [1–3].

Although many model-based methods act well in controlling systems, their performance degrades confronting disturbances and uncertainties. The reason is that these methods are entirely based on the system model and may lose their efficiency if there are unmodeled dynamics [4]. However, most robotic systems have uncertainty in the dynamic model and are also exposed to external disturbances. To solve this problem, a variety of research has been done to develop model-free controllers such as adaptive strategies, fuzzy methods, and neural network approaches [5–8].

Although model-free methods have many advantages and can reduce the impact of unmodulated dynamics on system behavior, some are developed based on measuring system states. However, in many practical applications, such as commercial robots, it is not possible to measure states such as velocity, and position is the only measurable state [9]. The reason is that adding velocity sensors such as tachometers increases the cost of hardware significantly. Adding tachometers may also change some parameters of the system. Moreover, one of the significant problems with dexterous arms is the hardness of integrating a large number of sensors within a small robot architecture, especially when the degrees of freedom are increased. Besides, speed measurement limits the available bandwidth of the system due to the presence of noise [10]. Some articles have calculated speed by differentiating the position of the joints. However, this solution is also not suitable because it causes the phenomenon of chattering in the consequent control input. The problem gets worse when the position signal is noisy. This phenomenon causes high-energy

© The Author(s), 2021. Published by Cambridge University Press.

https://doi.org/10.1017/S0263574721001120 Published online by Cambridge University Press

consumption at the actuators, which in turn reduces their lifetime and increases the failure rates. The application of low-pass filters on numerically calculated velocities, on the other hand, may degrade overall tracking performance. Furthermore, due to the system's nonlinearity, adjusting the filter parameters to ensure closed-loop stability is difficult and can only be accomplished through trial and error [11]. To deal with the problems caused by measuring and calculating the velocity state, observer-based methods for estimating velocity were presented. In [12], the problem of position/force trajectory tracking of robotic arms is settled based on an adaptive neural network controller. The proposed structure utilized a nonlinear observer to estimate the unmeasured velocity. In [13], an adaptive scheme is proposed for a 3-degree of freedom (DOF) manipulator based on the Slotine–Li control method. To this mean, an observer is developed to estimate velocity and force. The system stability is also proven. Shojaei et al. proposed an adaptive neural controller for manipulators, which is developed based on acceleration and velocity observer [14]. The boundedness of observation and control error signals are confirmed using the Lyapunov Theorem.

Given that uncertainty and disturbance are factors in the degradation of controller performance, many researchers have proposed methods to deal with them. In [15], a controller–observer scheme is presented for fault-tolerant control of a robotic arm utilizing the sliding mode approach. To this mean, a disturbance observer and a fuzzy approximation technique are integrated to approximate the disturbances and uncertainties. An adaptable super-twisting term is also considered in the control structure to enhance the disturbance rejection. In [16,17], robust controllers are designed for a multiagent system with uncertain Markovian chain topology. The system stability is verified using the Lyapunov lemmas. Hu et al. [18] proposed a dynamic surface control strategy for a flexible joint arm. A nonlinear observer is used to address the problem of disturbance estimation. Besides, a neuro-fuzzy scheme is presented to approximate the uncertainties. In [19], a controller is proposed for a robotic manipulator using the backstepping approach. Neural networks are utilized to estimate the unmodeled dynamics as well as disturbances. Stability analysis is also performed to confirm the boundedness of errors. In [20], an adaptive controller is introduced for a flexible-joint arm based upon the backstepping method. To estimate unknown dynamical terms, an approximator is proposed using fuzzy type 2. Haonan et al. [21] focused on solving the control issue of a specified form of nonlinear and uncertain systems such as manipulators. To this mean, an appointed-time method is developed based on neural networks and fuzzy logic. The states of the system, as well as the lumped uncertainty, are approximated utilizing a fuzzy wavelet neural network.

In addition to neural networks and fuzzy logic, other model-free approaches have been introduced to confront uncertainties and disturbances in dynamical systems. In this regard, the function approximation technique (FAT) is one of the practical approaches. FAT-based observers are mainly developed based upon Fourier series expansion [22–24], differential equations [25,26], and Baskakov operator [27]. In this article, an adaptive FAT-based controller–observer structure will be introduced for robotic manipulators. The motivation of adopting FAT-based approaches for designing the structure is the significant advantages of these approaches compared to both model-based and model-free neuro-fuzzy methods, which make them good candidates for dealing with disturbances and uncertainties [28]. These advantages are as follows: (1) In model-based control methods, change of parameters may affect the system performance significantly. Compared to these approaches, FAT-based methods are not dependent on system modeling. Therefore, the existence of unmodeled dynamics does not deteriorate their performance; (2) Designing systems based on fuzzy logic or neural networks require sufficient expertise to determine the parameters of the estimator/controller. Lack of enough experience will turn the design process into time-consuming and tedious work because it is necessary to determine the parameters based on trial and error. In FAT-based approaches, on the other hand, because of the simple structure and the limited number of parameters, their values can be easily determined; (3) In neuro-fuzzy systems, to keep the parameters in a particular range, projection algorithms are usually needed, which raises the computational load of the controller further; (4) Neuro-fuzzy structures usually require different feedbacks from system states. For example, when uncertainty is a function of system states, the neuro-fuzzy approximator needs to receive those states as inputs, which raise the computational complexity of the system.

https://doi.org/10.1017/S0263574721001120 Published online by Cambridge University Press

FAT-based estimators, on the other hand, approximate functions as time series and are not dependent on system states. This results in the reduction of system computational load.

In this article, the FAT is used to deal with unmodulated dynamics and disturbances so that the impact of these factors does not cause a decline in system performance. For this purpose, the Bernstein–Stancu polynomial is used to estimate of uncertainties and disturbances, and the coefficients of this polynomial are updated by developing adaptive rules. Stability analysis is carried out thoroughly using the Lyapunov theorem to confirm the boundedness of all errors. Finally, to evaluate the efficiency of the proposed adaptive FAT-based method, it is applied to a 2-DOF robotic arm, and the results are analyzed. The novelty and merits of the presented method are as follows: (1) Robust adaptive controller design using the Bernstein–Stancu Operator is a new idea in the robotics field; (2) The polynomial coefficients are adjusted using the adaptation law achieved in the stability analysis, while in previous related studies, the adaptive form of the Bernstein–Stancu Operator is not used; (3) The introduced controller is regressor-free. So, the problems of the usual adaptive methods do not appear in the proposed controller; (4) One of the advantages of the developed strategy is that there is no need to measure joint velocity, and joint position is the only measured state; (5) Moreover, in most of the previously developed robot controllers, the joint torque is used as the control signal, and actuator dynamics are neglected. However, as a more realistic presumption, in this work, actuator voltages are considered as the control signals.

Different sections of the article are as follows: The Bernstein–Stancu operator is described in Section 2. Section 3 reveals the manipulator dynamics. The adaptive FAT-based controller–observer is designed in Section 4. A thorough mathematical stability analysis is also performed in this section using the Lyapunov Theorem. The controller is simulated for the manipulator, and the results are presented in Section 5. Section 6 gives the most notable concluding remarks.

2. The Bernstein–Stancu Operator

The simplicity and ease of calculation make polynomials powerful mathematical tools that can be used to estimate different functions. It is also possible to estimate any complex and real-valued function with any degree of accuracy by combining several polynomials. A general class of linear and positive operators generalizing such well-known operators as those of Favard-Szasz, Bernstein, and Baskakov, was introduced by Stancu [29]. Stancu operators are described as follows. Consider $m \geq 1$ and $p \geq 0$ as natural numbers and suppose f be in $C\left[0, 1 + \frac{p}{m}\right]$. We denote by $C\left[0, 1 + \frac{p}{m}\right]$, the set of continuous functions on $\left[0, 1 + \frac{p}{m}\right]$. The natural numbers m and p are used to determine the upper bound of this interval. Moreover, consider α, β and γ are positive constants that satisfy $0 \leq \beta \leq \gamma$ and $\alpha \geq 0$. Then, the Bernstein–Stancu Operators are given by the following equation:

$$L_{mp}^{<\alpha,\beta,\gamma>}(f,t) = \sum_{k=0}^{m+p} \binom{m+p}{k} \frac{t^{(k,-\alpha)}(1-t)^{(m+p-k,-\alpha)}}{1^{(m+p,-\alpha)}} f\left(\frac{k+\beta}{m+\gamma}\right) \tag{1}$$

In Eq. (1), $\binom{m+p}{k}$ denotes the binomial coefficient, which is described as

$$\binom{m+p}{k} = \frac{(m+p)!}{(m+p-k)!k!} \tag{2}$$

The k th order factorial power with increment $(-\alpha)$ of t is shown by $t^{(k,-\alpha)}$, which is described as

$$t^{(k,-\alpha)} = \begin{cases} \prod_{v=0}^{k-1} (t + v\alpha) & \text{if k} \geq 1 \text{ and t} > 0 \\ 1 & \text{else} \end{cases} \tag{3}$$

Thus, if $t \in [0, 1]$ and $\alpha \geq 0$, then one can conclude that $L_{mp}^{<\alpha,\beta,\gamma>}$ is a linear and positive operator. In [29], it has been proved that if $f \in [0, 1]$ and $0 \leq \alpha = \alpha_{m+p} \to 0$ as $m + p \to \infty$, then the sequence

https://doi.org/10.1017/S0263574721001120 Published online by Cambridge University Press

$\left\{L_{mp}^{<\alpha,\beta,\gamma>}(f,t)\right\}$ converges to $f(t)$ uniformly on [0, 1]. It is straightforward to present that:

$$L_{mp}^{<\alpha,\beta,\gamma>}(f,t) = W_f^T Z_f \tag{4}$$

in which

$$W_f = \left[f\left(\frac{\beta}{m+\gamma}\right)(m+p)f\left(\frac{1+\beta}{m+\gamma}\right)\frac{(m+p)(m+p-1)}{2!}f\left(\frac{2+\beta}{m+\gamma}\right)\ldots f\left(\frac{m+p+\beta}{m+\gamma}\right)\right]^T \in \Re^N \tag{5}$$

Is a vector consisting of adjustable parameters, and the number of chosen basis functions is $N = m + p + 1$, and the basis functions vector is

$$Z_f = \left[\frac{(1-t)^{(m+p,-\alpha)}}{1^{(m+p,-\alpha)}}\frac{t^{(1,-\alpha)}(1-t)^{(m+p-1,-\alpha)}}{1^{(m+p,-\alpha)}}\frac{t^{(2,-\alpha)}(1-t)^{(m+p-2,-\alpha)}}{1^{(m+p,-\alpha)}}\ldots\frac{t^{(m+p,-\alpha)}}{1^{(m+p,-\alpha)}}\right]^T \in \Re^N \tag{6}$$

In other words, (4) can be used as a linear form of (1). Using linear form of these equations is more common in adaptive control.

3. Robot Dynamic Modeling

Suppose an n-DOF robotic arm, which is driven by n DC actuators. The motion behavior of the actuators is modeled by the following equations [30].

$$J_m\frac{d^2\theta}{dt^2} + (b_m + k_m k_b R^{-1})\frac{d\theta}{dt} = k_m R^{-1}u(t) - r\tau_l \tag{7}$$

where angular positions of actuators are represented by the vector $\theta \in \Re^n$. $J_m \in \Re^{n\times n}[kg.m^2]$, which is a diagonal matrix, consists of transmission elements of the motor side and the rotor inertias. The diagonal matrix $b_m \in \Re^{n\times n}[N.m.s/rad]$ comprises transmission elements of motor side and motor damping coefficients. Actuator–torque constants are denoted by the diagonal matrix $k_m \in \Re^{n\times n}[N.m/A]$. The back-Electromotive force (EMF) constants are represented by $k_b \in \Re^{n\times n}[N.m/A]$, which is a diagonal matrix. $R \in \Re^{n\times n}[\Omega]$ is the armature resistances diagonal matrix. The voltages applied to the joint motors are denoted by $u(t) \in \Re^n[v]$. The load torques are shown by the vector $\tau_l \in \Re^n[N.m]$. The $n \times n$ transmission matrix r is utilized to map $\dot{\theta}$ (the vector of actuator coordinate velocities) to $\dot{q}$ (the vector of joint velocities), as

$$\dot{q} = r\dot{\theta} \tag{8}$$

The dynamic model of a manipulator represents its motion and is formed based on the Euler–Lagrange equation. That is to say, first, the Lagrangian is formed as the difference between the kinetic and the potential energies of the system. Further manipulations of the Lagrangian leads to the dynamic equation of a rigid n-DOF robotic arm, described as (9). The complete procedure of deriving the dynamic model of the arms is explained in [31].

$$D(q)\ddot{q} + C(q,\dot{q})\dot{q} + g(q) + T_l(t) = \tau_l \tag{9}$$

where, the joint acceleration, velocity, and position are denoted by $n\times 1$ vectors $\ddot{q}$, $\dot{q}$, and q, respectively. $D(q) \in \Re^{n\times n}$ is a positive-definite and symmetric matrix. $C(q,\dot{q})\dot{q} \in \Re^n$ is the vector of Coriolis/centrifugal forces, $g(q) \in \Re^n$ is the vector of gravitational forces, and $T_l(t) \in \Re^n$ is the vector of external disturbance. It is easy to show that the integrated actuator–manipulator model can be formulated as follows:

$$\ddot{q} = u(t) + \eta(t) \tag{10}$$

https://doi.org/10.1017/S0263574721001120 Published online by Cambridge University Press

Where $\eta(t) = \left(-M^{-1}(q)(V_m(q,\dot{q})\dot{q} + H(q,\dot{q})) + (M^{-1}(q)r^{-1}k_m R^{-1} - I_n)u(t)\right) \in \Re^n$ represents the lumped uncertainty vector inserted to the system dynamic, and

$$M(q) = D(q) + r^{-1}J_m r^{-1}$$
$$V_m(q,\dot{q}) = C(q,\dot{q}) + r^{-1}(b_m + k_m k_b R^{-1})r^{-1}$$
$$H(q,\dot{q}) = G(q) + T_l(t)$$

4. The Designed Controller–Observer Scheme

The error of tracking is considered as $e(t) = q(t) - q_d(t) \in \Re^n$, where the joint space desired path is represented by $q_d \in \Re^n$. So, Eq. (10) is rewritten as follows.

$$\ddot{e} = u(t) - \ddot{q}_d + \eta(t) \tag{11}$$

To address the trajectory tracking problem for (11) using position feedback only, consider the following control input and observer dynamics:

$$u(t) = -K_d\dot{\hat{e}} - K_p\hat{e} + \ddot{q}_d - \hat{\eta}(t) \tag{12}$$

$$\begin{cases} \dot{\hat{e}} = \rho + L_d(e - \hat{e}) \\ \dot{\rho} = L_p(e - \hat{e}) \end{cases} \tag{13}$$

Where $K_d \in \Re^{n\times n}$ and $K_p \in \Re^{n\times n}$ are positive-definite diagonal gain matrices; $\hat{e}(t) = \hat{q}(t) - q_d(t)$ is the approximation of $e(t)$; $L_d \in \Re^{n\times n}$ and $L_p \in \Re^{n\times n}$ are diagonal and positive observer gain matrices, and $\hat{\eta}(t)$ represents the estimation of $\eta(t)$. The following assumption is considered on the structure of K_p, K_d, L_d, and L_p.

Assumption 1: K_p, K_d, L_d and L_p satisfy the following equations.

$$K_p = \mu K_d \tag{14}$$

$$K_d = (k_d + \gamma)I_n \tag{15}$$

$$L_p = \mu l_d I_n \tag{16}$$

$$L_d = (l_d + \mu)I_n \tag{17}$$

Where μ, k_d, γ and l_d are positive constants, $k_d > \mu$, and I_n shows the identity matrix of dimension n. Substituting (12) into (11) and using definition (14) yields

$$\ddot{e} = -K_d\dot{\hat{e}} - \mu K_d\hat{e} + \eta(t) - \hat{\eta}(t) \tag{18}$$

Define

$$s_1(t) = \dot{e}(t) + \mu e(t) \tag{19}$$

$$s_2(t) = \dot{q}(t) - \dot{q}_0(t) \tag{20}$$

Where $\dot{q}_0(t) = \dot{\hat{q}}(t) - \mu\tilde{q}(t)$ and

$$\tilde{q}(t) = e(t) - \hat{e}(t) = q(t) - \hat{q}(t) \tag{21}$$

https://doi.org/10.1017/S0263574721001120 Published online by Cambridge University Press

denotes the joint position estimation error. So, the closed-loop error dynamic is achieved as

$$\ddot{e} = -K_d s_1 + K_d s_2 + \eta(t) - \hat{\eta}(t) \tag{22}$$

$$\dot{s}_2 + (l_d I_n - K_d)s_2 = -K_d s_1 + \eta(t) - \hat{\eta}(t) \tag{23}$$

where we have utilized (20) and the following equality

$$\ddot{q}_0(t) - \ddot{q}_d(t) = l_d s_2(t) \tag{24}$$

Now, $\eta(t)$ is represented using the basis functions in a linear form based upon the universal approximation theorem as

$$\eta(t) = W_\eta^T Z_\eta + \varepsilon_\eta \tag{25}$$

where the number of used basis functions is denoted by N_1 and the ideal weighting vector is presented by $W_\eta \in \Re^{nN_1 \times n}$. The approximation errors are represented by ε_η, and $Z_\eta \in \Re^{nN_1}$ is the basis functions vector. Using the same basis functions set, we propose

$$\hat{\eta}(t) = \hat{W}_\eta^T Z_\eta \tag{26}$$

In this equation, $\hat{W}_\eta \in \Re^{nN_1 \times n}$ is the approximation of W_η. Equations (25) and (26) are integrated into (22) and (23) to achieve

$$\ddot{e} = -K_d s_1 + K_d s_2 + \tilde{W}_\eta^T Z_\eta + \varepsilon_\eta \tag{27}$$

$$\dot{s}_2 + (l_d I_n - K_d)s_2 = -K_d s_1 + \tilde{W}_\eta^T Z_\eta + \varepsilon_\eta \tag{28}$$

where the Bernstein–Stancu Operator weight approximation error is denoted by $\tilde{W}_\eta = W_\eta - \hat{W}_\eta$.

4.1 Stability analysis

The following Lyapunov candidate is proposed to analyze the system stability,

$$V(x, \tilde{W}_\eta) = \frac{1}{2} x^T P x + \frac{1}{2} Tr(\tilde{W}_\eta^T \Gamma_\eta \tilde{W}_\eta) \tag{29}$$

where

$$x = \begin{bmatrix} \dot{e}^T & (\mu e)^T & \dot{\tilde{q}}^T & (\mu \tilde{q})^T \end{bmatrix}^T \in \Re^{4n} \tag{30}$$

$$P = \begin{bmatrix} \begin{bmatrix} I_n & I_n \\ I_n & 2\mu^{-1} k_d I_n \end{bmatrix} & 0_{2n} \\ 0_{2n} & \begin{bmatrix} I_n & I_n \\ I_n & 2\mu^{-1} k_d I_n + I_n \end{bmatrix} \end{bmatrix} \in \Re^{4n \times 4n} \tag{31}$$

With 0_{2n} denoting the null matrix of dimension $2n$; $\Gamma_\eta \in \Re^{nN_1 \times nN_1}$ is a positive-definite matrix and is $Tr(\cdot)$ the trace operator.

Lemma 1: *The upper and lower bounds of (29) are as follows,*

$$V(x, \tilde{W}_\eta) \leq \frac{1}{2} \bar{\lambda}(P) \|x\|^2 + \frac{1}{2} \bar{\lambda}(\Gamma_\eta) Tr(\tilde{W}_\eta^T \tilde{W}_\eta) \tag{32}$$

$$V(x, \tilde{W}_\eta) \geq \frac{1}{2} \underline{\lambda}(P) \|x\|^2 + \frac{1}{2} \underline{\lambda}(\Gamma_\eta) Tr(\tilde{W}_\eta^T \tilde{W}_\eta) \tag{33}$$

https://doi.org/10.1017/S0263574721001120 Published online by Cambridge University Press

With $\bar{\lambda}(P)$ and $\underline{\lambda}(P)$ are defined as

$$\bar{\lambda}(P) = 6\mu^{-1}k_d, \quad \underline{\lambda}(P) = \frac{1}{3} \tag{34}$$

Proof: Introducing

$$y^T = \begin{bmatrix} s_1^T(\mu e)^T & s_2^T(\mu\tilde{q})^T \end{bmatrix} \tag{35}$$

Function (29) could be rewritten as

$$V(y, \tilde{W}_\eta) = \frac{1}{2}y^T\Lambda y + \frac{1}{2}Tr(\tilde{W}_\eta^T\Gamma_\eta\tilde{W}_\eta) \tag{36}$$

where

$$\Lambda = \begin{bmatrix} \begin{bmatrix} I_n & 0_n \\ 0_n & 2\mu^{-1}k_dI_n - I_n \end{bmatrix} & 0_{2n} \\ 0_{2n} & \begin{bmatrix} I_n & 0_n \\ 0_n & 2\mu^{-1}k_dI_n \end{bmatrix} \end{bmatrix} \in \Re^{4n\times 4n} \tag{37}$$

It is not difficult to demonstrate that

$$\begin{aligned} &\tfrac{1}{2}(\underline{\lambda}(\Lambda)\|y\|^2 + \underline{\lambda}(\Gamma_\eta)Tr(\tilde{W}_\eta^T\tilde{W}_\eta)) \leq \\ &V(y, \tilde{W}_\eta) \leq \tfrac{1}{2}(\bar{\lambda}(\Lambda)\|y\|^2 + \bar{\lambda}(\Gamma_\eta)Tr(\tilde{W}_\eta^T\tilde{W}_\eta)) \end{aligned} \tag{38}$$

where

$$\underline{\lambda}(\Lambda) = 1, \quad \bar{\lambda}(\Lambda) = 2\mu^{-1}k_d \tag{39}$$

By definition

$$y = Tx \tag{40}$$

using (30) and

$$T = \begin{bmatrix} \begin{bmatrix} I_nI_n \\ 0_nI_n \end{bmatrix} & 0_{2n} \\ 0_{2n} & \begin{bmatrix} I_n & I_n \\ 0_n & I_n \end{bmatrix} \end{bmatrix} \tag{39}$$

It can be easily shown that

$$\frac{1}{3}\|x\|^2 \leq \|y\|^2 \leq 3\|x\|^2 \tag{42}$$

Together with (38) and (39), it implies (32)–(34) □

It is worthy of mentioning that similar proof approaches are revealed in [32]. Differentiating (29) over time, using (15), (27), (28), and rearranging with some mathematical simplification, we have

$$\begin{aligned} \dot{V}(x, \tilde{W}_\eta) = &\underbrace{-s_1^Tk_dI_ns_1 + \dot{e}^T\mu I_n\dot{e} - s_2^Tk_dI_ns_2 + 2e^T\mu k_dI_n\dot{e} + 2\tilde{q}^T\mu k_dI_n\dot{\tilde{q}}}_{\wp} \\ &- s_1^T\gamma I_ns_1 - s_2^T\gamma I_ns_2 - s_2^T(l_dI_n - 2K_d)s_2 + (s_1^T + s_2^T)\varepsilon_\eta \\ &+ (s_1^T + s_2^T)\tilde{W}_\eta^TZ_\eta - Tr(\tilde{W}_\eta^T\Gamma_\eta\dot{\hat{W}}_\eta) \end{aligned} \tag{43}$$

It is straightforward to show that the five first terms of Eq. (43) can be simplified as $\wp = -\dot{e}^Tk_dI_n\dot{e} - e^T\mu k_dI_n\mu e + \dot{e}^T\mu I_n\dot{e} - \dot{\tilde{q}}^Tk_dI_n\dot{\tilde{q}} - \tilde{q}^T\mu k_dI_n\mu\tilde{q}$. Thus, Eq. (43) is written as

$$\begin{aligned} \dot{V}(x, \tilde{W}_\eta) = &-x^TQx - s_1^T\gamma I_ns_1 - s_2^T\gamma I_ns_2 - s_2^T(l_dI_n - 2K_d)s_2 \\ &+ (s_1^T + s_2^T)\varepsilon_\eta - Tr(\tilde{W}_\eta^T(\Gamma_\eta\dot{\hat{W}}_\eta - Z_\eta(s_1^T + s_2^T))) \end{aligned} \tag{44}$$

https://doi.org/10.1017/S0263574721001120 Published online by Cambridge University Press

where

$$Q=\begin{bmatrix}\begin{bmatrix}(k_d-\mu)I_n & 0_n\\ 0_n & k_dI_n\end{bmatrix} & \begin{matrix}0_{2n}\end{matrix}\\ \begin{matrix}0_{2n}\end{matrix} & \begin{bmatrix}k_dI_n & 0_n\\ 0_n & k_dI_n\end{bmatrix}\end{bmatrix}\in\Re^{4n\times 4n} \tag{45}$$

By selecting the updating laws as:

$$\hat{W}_\eta=2\Gamma_\eta^{-1}(Z_\eta q-\int \dot{Z}_\eta q^T dt)+\Gamma_\eta^{-1}\int Z_\eta\aleph dt-\sigma_\eta\Gamma_\eta^{-1}\int \hat{W}_\eta dt \tag{46}$$

in which

$$\aleph=-\dot{q}_d^T+\mu e^T-\dot{\hat{q}}^T+\mu\tilde{q}^T \tag{47}$$

and σ_η is a positive number, (44) is simplified as

$$\begin{aligned}\dot{V}(x,\tilde{W}_\eta)\le&-\underline{\lambda}(Q)\|x\|^2-\gamma\|s_1\|^2-\gamma\|s_2\|^2+\|s_1\|\left\|\varepsilon_\eta\right\|+\|s_2\|\left\|\varepsilon_\eta\right\|\\&+\sigma_\eta Tr(\tilde{W}_\eta^T\hat{W}_\eta)\end{aligned} \tag{48}$$

where, we have utilized the fact that $l_dI_n-2K_d>0$. Using the relation $\|s_1\|,\|s_2\|\le\|y\|\le\sqrt{3}\|x\|$, the last inequality is further simplified,

$$\dot{V}(x,\tilde{W}_\eta)\le-\underline{\lambda}(Q)\|x\|^2+2\sqrt{3}\|x\|\left\|\varepsilon_\eta\right\|+\sigma_\eta Tr(\tilde{W}_\eta^T\hat{W}_\eta) \tag{49}$$

Result 1: Assume that enough basis functions are utilized for estimation so that the estimation error is negligible. Hence, the term σ-modification can be neglected in (46). As a result,

$$\dot{V}(x,\tilde{W}_\eta)\le-\underline{\lambda}(Q)\|x\|^2 \tag{50}$$

Therefore, the vector x converges to zero asymptotically.

Result 2: Assume that ε_η in (49) is not negligible. It is not difficult to show that (51) holds.

$$-\underline{\lambda}(Q)\|x\|^2+2\sqrt{3}\|x\|\left\|\varepsilon_\eta\right\|\le-0.5\underline{\lambda}(Q)\|x\|^2+\frac{6}{\underline{\lambda}(Q)}\left\|\varepsilon_\eta\right\|^2 \tag{51}$$

$$2Tr(\tilde{W}_\eta^T\hat{W}_\eta)\le Tr(W_\eta^TW_\eta)-Tr(\tilde{W}_\eta^T\tilde{W}_\eta) \tag{52}$$

Regarding these equations, (49) is written as

$$\dot{V}(x,\tilde{W}_\eta)\le-0.5\underline{\lambda}(Q)\|x\|^2-0.5\sigma_\eta Tr(\tilde{W}_\eta^T\tilde{W}_\eta)+\frac{6}{\underline{\lambda}(Q)}\left\|\varepsilon_\eta\right\|^2+0.5\sigma_\eta Tr(W_\eta^TW_\eta) \tag{53}$$

Considering (32), one can easily relate (53) to V as follows

$$\begin{aligned}\dot{V}(x,\tilde{W}_\eta)\le&-\omega V+0.5\left(\omega\bar{\lambda}(P)-\underline{\lambda}(Q)\right)\|x\|^2+\frac{6}{\underline{\lambda}(Q)}\left\|\varepsilon_\eta\right\|^2\\&+0.5\left(\omega\bar{\lambda}(\Gamma_\eta)-\sigma_\eta\right)Tr(\tilde{W}_\eta^T\tilde{W}_\eta)+0.5\sigma_\eta Tr(W_\eta^TW_\eta)\end{aligned} \tag{54}$$

Now, by choosing ω as

$$\omega\le\min\left\{\frac{\underline{\lambda}(Q)}{\bar{\lambda}(P)},\frac{\sigma_\eta}{\bar{\lambda}(\Gamma_\eta)}\right\} \tag{55}$$

Equation (54) is simplified to

$$\dot{V}(x,\tilde{W}_\eta)\le-\omega V+\frac{6}{\underline{\lambda}(Q)}\left\|\varepsilon_\eta\right\|^2+0.5\sigma_\eta Tr(W_\eta^TW_\eta) \tag{56}$$

https://doi.org/10.1017/S0263574721001120 Published online by Cambridge University Press

This means that $\dot{V}(x, \tilde{W}_\eta)$ is negative-definite, whenever:

$$(x, \tilde{W}_\eta) \in \Omega \equiv \left\{ (x, \tilde{W}_\eta) \left| V > \frac{6}{\omega \underline{\lambda}(Q)} \sup_{t_0 \leq \tau} \left\| \varepsilon_\eta(\tau) \right\|^2 + \frac{1}{2\omega} \sigma_\eta Tr(W_\eta^T W_\eta) \right. \right\} \tag{57}$$

As a result, the uniformly ultimately boundedness of x and $\tilde{W}_\eta$ is proved. This indicates that the set Ω size is tunable by choosing the ω, σ_η and Q parameters properly.

4.2. Performance assessment

To ensure the proper performance of the introduced controller–observer structure, in response to the initial conditions, (56) is solved to achieve,

$$V(t) \leq V(t_0) e^{-\omega(t-t_0)} + \frac{6}{\omega \underline{\lambda}(Q)} \sup_{t_0 < \tau < t} \left\| \varepsilon_\eta(\tau) \right\|^2 + \frac{1}{2\omega} \sigma_\eta Tr(W_\eta^T W_\eta) \tag{58}$$

Considering (33), which presents the lower bound of (29), one can conclude that,

$$\|x\| \leq \sqrt{\frac{2V}{\underline{\lambda}(P)}} \tag{59}$$

That is simplified to (60) by employing (58)

$$\begin{aligned} \|x\| \leq & \sqrt{\frac{2V(t_0)}{\underline{\lambda}(P)}} e^{-0.5\omega(t-t_0)} + \sqrt{\frac{12}{\omega \underline{\lambda}(P) \underline{\lambda}(Q)}} \sup_{t_0 < \tau < t} \left\| \varepsilon_\eta(\tau) \right\| \\ & + \frac{1}{\sqrt{\omega \underline{\lambda}(P)}} [\sigma_\eta Tr(W_\eta^T W_\eta)]^{\frac{1}{2}} \end{aligned} \tag{60}$$

which indicates the amplitude $\|x\|$ boundedness, where the bound is the summation of exponential functions and constants.

5. Simulation Results

5.1. The testbed system details

A manipulator with two revolute joints is considered as a testbed to evaluate the proposed adaptive FAT-based controller. Eq. (9) indicates the robot dynamics, and the matrices are defined as [33,34],

$$\begin{aligned} D(q) &= \begin{bmatrix} d_{11} & d_{12} \\ d_{21} & d_{22} \end{bmatrix} \\ d_{11} &= m_1 l_{c1}^2 + I_1 + m_2 (l_1^2 + l_{c2}^2 + 2 l_1 l_{c2} cos(q_2)) + I_2 \\ d_{21} &= d_{12} = m_2 l_{c2}^2 + m_2 l_1 l_{c2} cos(q_2) + I_2 \\ d_{22} &= m_2 l_{c2}^2 + I_2 \\ C(q, \dot{q})\dot{q} &= \begin{bmatrix} -2 m_2 l_1 l_{c2} sin(q_2)(\dot{q}_1 \dot{q}_2 + 0.5 \dot{q}_2^2) \\ m_2 l_1 l_{c2} sin(q_2) \dot{q}_1^2 \end{bmatrix} \\ g(q) &= \begin{bmatrix} m_1 l_{c1} g cos(q_1) + m_2 g (l_{c2} cos(q_1 + q_2) + l_1 g cos(q_1)) \\ m_2 l_{c2} g cos(q_1 + q_2) \end{bmatrix} \end{aligned} \tag{61}$$

where each joint angle is denoted by q_i and l_i is the length of each link. The length and mass of the first link are considered as $l_1 = 0.4318$ m and m_1=3 kg, respectively, and the second link counterparts are $l_2 = 0.6491$ m and $m_2 = 1$ kg, respectively. The exact values of motor model parameters are set to R=diag(1,1), J_m=diag(10^{-6},10^{-6}), r=diag(0.01, 0.01), $K_m = K_b$=diag(0.03,0.03), and

https://doi.org/10.1017/S0263574721001120 Published online by Cambridge University Press

b_m=diag(10^{-4},10^{-4}). The initial joint angles are assumed as $q = \begin{bmatrix} 0.0691 & 1.4326 \end{bmatrix}^{\mathrm{T}}(rad)$, and the aim is to track a desired sinusoidal trajectory for 1 s. It is presumed that the initial values of the actual and desired angles are the same. It is supposed that information on the matrices $g(q)$, $C(q,\dot{q})$ and $D(q)$ is unavailable. The numerical values of the controller–observer structure are $l_d = 45$, $\gamma = 5$, $k_d = 15$ and $\mu = 10$. To approximate the lumped uncertainty $\eta(t)$, the first three terms of the Bernstein–Stancu polynomial are chosen. So, $\hat{W}_\eta \in \Re^{6\times 2}$, the adaptive parameters are initiated at zero. The convergence rate matrix is chosen as $\Gamma_\eta = 10^{-3} \times I_6$, where I_6 is the 6×6 identity matrix. At this point, suppose that the estimation error is small and therefore negligible.

To investigate the efficiency of the proposed FAT-based approximator, its performance is compared with other estimators. For this purpose, the Radial Basis Function Neural Network (RBFNN) and fuzzy system, as two state-of-art approximators, are integrated into the presented controller to estimate the external disturbances and the uncertainties. These methods are described in the following subsections.

5.2. First compared method: the RBFNN uncertainty approximator

To compare the results of the proposed technique and the RBFNN uncertainty approximator, both methods are integrated into the designed controller. RBFNN is used to estimate the uncertainties and external disturbances. The output of RBFNN is computed by a linear combination of hidden layer outputs of the neural network. Assume that the RBFNN inputs are the elements of the vector $\varpi_j(t) = \begin{bmatrix} \hat{e}_j(t) & \dot{\hat{e}}_j(t) \end{bmatrix}$ for j = 1,2. Consequently,

$$Z_\eta = \begin{bmatrix} \xi_1 & \xi_2 & \dots & \xi_{N_1} \end{bmatrix}^T \in \Re^{N_1} \tag{62}$$

$$\xi_i = \exp\left(-\frac{\left\|\varpi_j(t) - c_i\right\|^2}{\delta_i^2}\right) \quad i = 1, 2, \dots, N_1 \tag{63}$$

where N_1 denotes the number of neurons in the hidden layer. The initial weights of the RBFNN are set to zero. The controller parameters are set equal to the previously stated values. The values of c_i and δ_i are set to

$$\begin{gathered} c_1 = \begin{bmatrix} -2\times 10^{-2} \\ -4.5 \end{bmatrix}, c_2 = \begin{bmatrix} -1.6\times 10^{-3} \\ -3.6 \end{bmatrix}, c_3 = \begin{bmatrix} -1.2\times 10^{-3} \\ -2.7 \end{bmatrix}, c_4 = \begin{bmatrix} -8\times 10^{-3} \\ -1.8 \end{bmatrix} \\ c_5 = \begin{bmatrix} -4\times 10^{-2} \\ -0.9 \end{bmatrix}, c_6 = \begin{bmatrix} 0 \\ 0 \end{bmatrix} \end{gathered} \tag{64}$$

$$\delta_1 = 4,\ \delta_2 = 3,\ \delta_3 = 2,\ \delta_4 = 2,\ \delta_5 = 1,\ \delta_6 = 0.5 \tag{65}$$

These values are achieved by trial and error and are not optimally chosen.

5.3. Second compared method: the fuzzy system

To compare the results, another form of the presented approach is utilized, which is established based on the fuzzy approximator instead of the Bernstein–Stancu polynomials approximator to estimate the nonlinear function $\eta(t)$. Consider the $x_1 = q(t)$ and $x_2 = \dot{q}(t)$ as the inputs of the fuzzy system. Three membership functions are considered for each fuzzy input. Consequently, there are nine fuzzy rules. Consider the linguistic fuzzy rules as

$$\text{Rule } l\text{:if } x_1 \text{ is } A_l \text{ and } x_2 \text{ is } B_l \text{ Then } \hat{\eta}(t) \text{ is } D_l \tag{66}$$

in which Rule l shows the lth fuzzy rule for $l = 1,\dots,9$. In the lth rule, the fuzzy variables x_1, x_2 and $\hat{\eta}(t)$, will be evaluated by the fuzzy membership functions A_l, B_l and D_l. Three membership functions P, Z,

https://doi.org/10.1017/S0263574721001120 Published online by Cambridge University Press

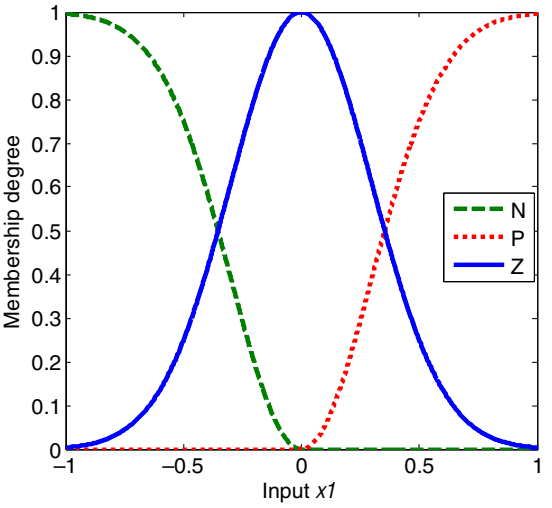


Figure 1. *Membership functions for the inputs* x_1.

and N are considered for the inputs x_1 and x_2 in the system operating space. The mathematic equations of the membership functions for the input x_1 are

$$\begin{aligned}\mu_N(x_1) &= \begin{cases} 0 & x > 0 \\ 1-\mu_Z(x_1) & x \le 0 \end{cases}, \\ \mu_P(x_1) &= \begin{cases} 0 & x < 0 \\ 1-\mu_Z(x_1) & x \ge 0 \end{cases}, \\ \mu_Z(x_1) &= \exp\left(-\frac{x_1^2}{2\sigma^2}\right), \sigma = 0.3 \end{aligned} \tag{67}$$

These functions are plotted in Fig. 1. Similarly, the membership functions for the input x_2 will be defined. Also, the membership functions for the output $\hat{\eta}(t)$ are in the form of

$$\mu_{D_l}(\hat{\eta}) = \exp\left(-\frac{(\hat{\eta}-\hat{y}_l)^2}{2\sigma^2}\right) \tag{68}$$

in which $\hat{y}_l$ is the center of D_l. According to [5], $\hat{\eta}$ can be represented as

$$\hat{\eta} = \sum_{l=1}^{9} \hat{y}_l \psi_l(x_1,x_2) = \hat{y}^T \psi(x_1,x_2) \tag{69}$$

Where $\hat{y} = [\,\hat{y}_1 \ldots \hat{y}_9\,]^T$ and $\psi = [\,\psi_1 \ldots \psi_9\,]^T$ in which ψ_l is a positive value expressed as

$$\psi_l(x_1,x_2) = \frac{\mu_{A_l}(x_1)\mu_{B_l}(x_2)}{\sum_{l=1}^{9} \mu_{A_l}(x_1)\mu_{B_l}(x_2)} \tag{70}$$

The controller settings used for the fuzzy system are the same as before, except for $\Gamma_\eta = 10^{-3} \times I_9$.

5.4. Results: performance evaluation and comparison

To evaluate the robustness of the proposed schemes, external disturbances and payload variations are considered. Suppose that, during the trajectory tracking, a heavy load is picked up by the second link at $t = 0.4$ s and is released at $t = 0.7$ s. The picked payload can be considered as a part of the second link,

https://doi.org/10.1017/S0263574721001120 Published online by Cambridge University Press

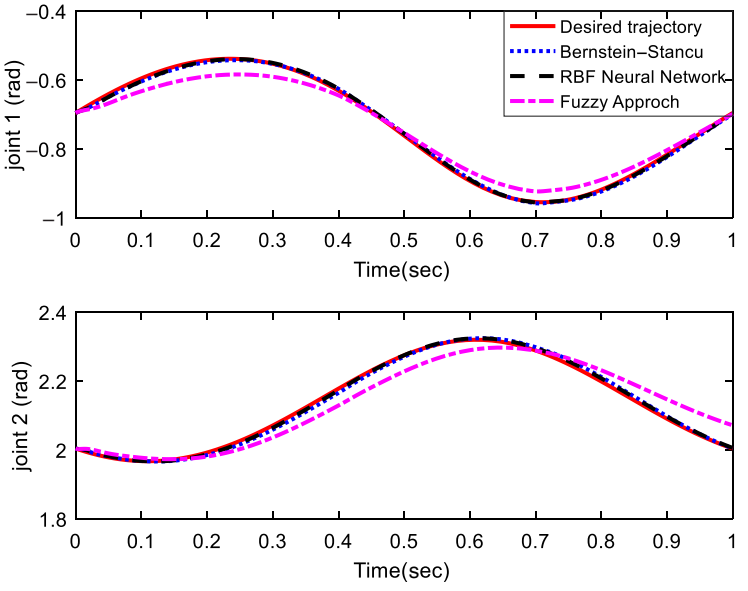


Figure 2. *The desired and actual paths.*

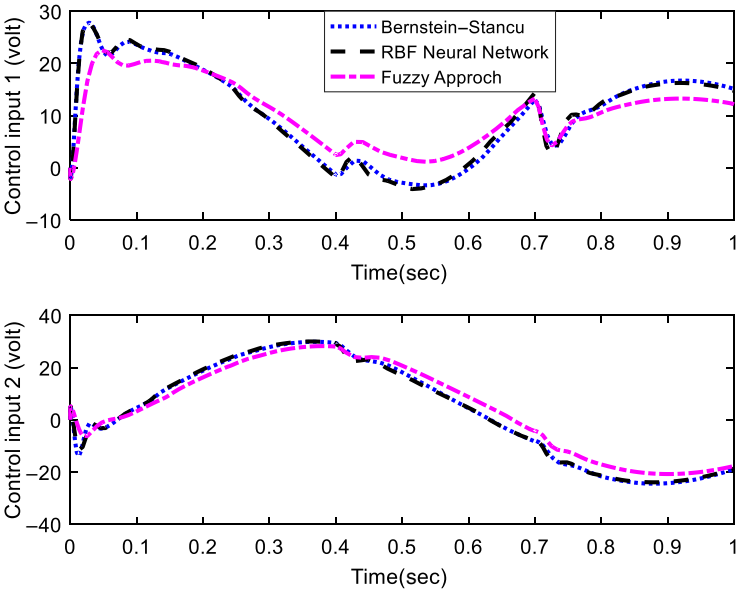


Figure 3. *Control signals.*

so, there is a variation in the link mass at $t = 0.4$ s, and it becomes $m_2 + \Delta m_2$, and the load is eliminated at $t = 0.7$ s. It is assumed that $\Delta m_2 = 8$ kg. Besides, the external disturbance is considered as

$$T_l(t) = \begin{bmatrix} 24\sin\left(\dfrac{5\pi t}{4}\right) + 16\sin(1.8\pi t) + 24 \\ 24\sin\left(\dfrac{5\pi t}{4}\right) + 16\sin(1.8\pi t) + 24 \end{bmatrix} \tag{71}$$

Under these settings, the proposed controller–observer is applied to the robot along with the RBFNN and fuzzy approximator-based controllers. Figure 2 illustrates the desired and actual paths regarding these methods. According to the figure, despite external disturbances and uncertainties, the manipulator

https://doi.org/10.1017/S0263574721001120 Published online by Cambridge University Press

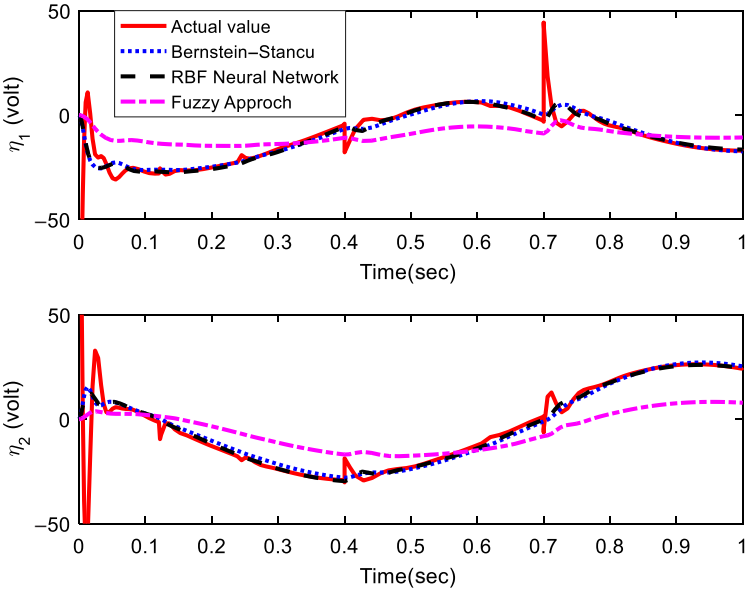


Figure 4. *The estimation performance of $\eta(t)$.*

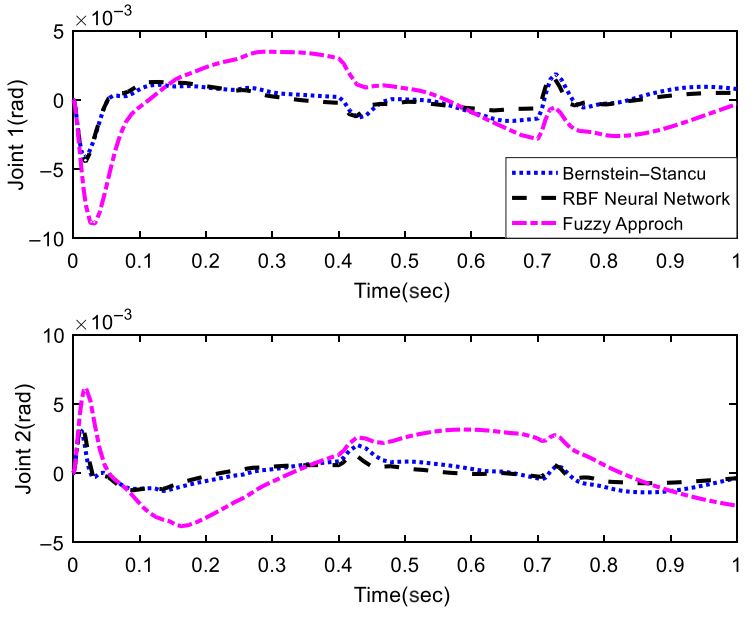


Figure 5. *The joint position estimation errors for joints 1 and 2.*

is capable of fulfilling successful trajectory tracking. The results also indicate the signals boundedness. This figure illustrates that the performances of both RBFNN and the Bernstein–Stancu-based approach are nearly the same because of the universal approximation property of RBFNN and Bernstein–Stancu polynomials. On the other hand, the proposed method outperforms the fuzzy approximator significantly. Figure 3 illustrates the control signals employed to the joint motors by different controller–observer structures. According to this figure, the control signals are smooth and bounded for all applied methods. Figure 4 reveals the approximated lumped uncertainties. Based on the figure, the proposed FAT-based strategy and the RBFNN method are capable of good uncertainty estimation. The fuzzy approximator,

https://doi.org/10.1017/S0263574721001120 Published online by Cambridge University Press

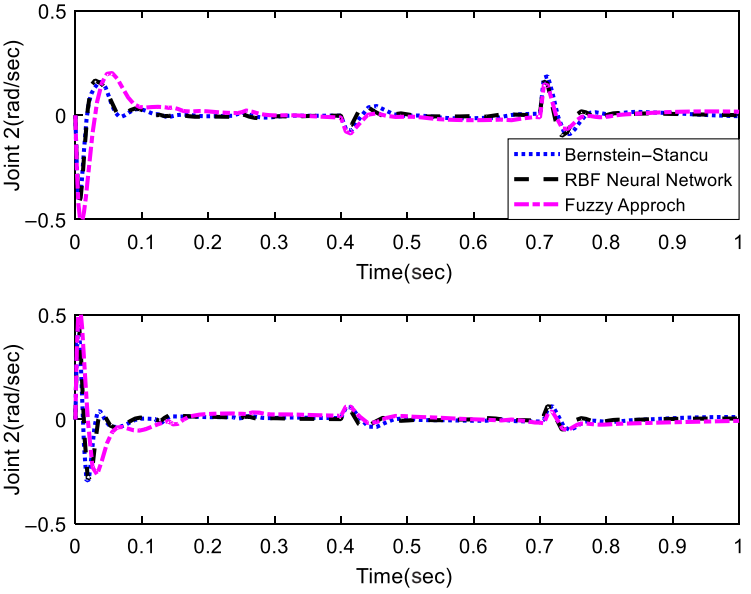


Figure 6. *The joint velocity estimation errors for joints 1 and 2.*

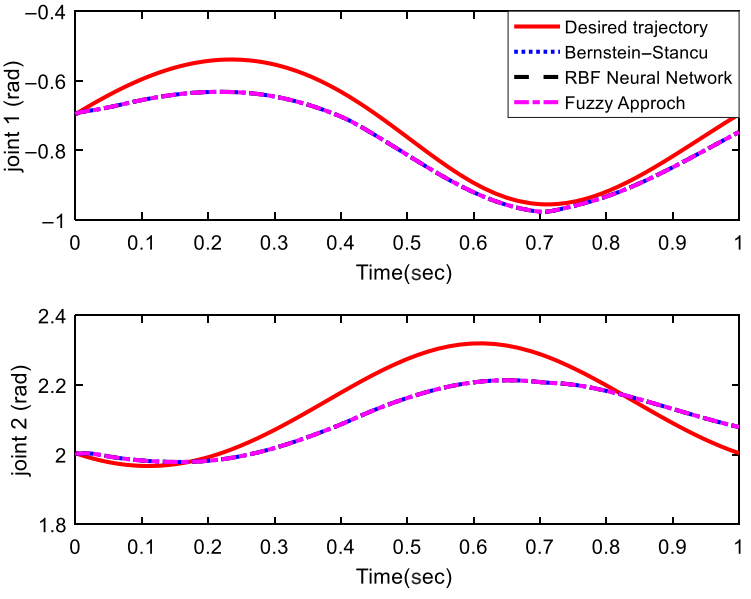


Figure 7. *The desired and actual paths in the absence of* $\hat{\eta}(t)$.

on the other hand, fails to fulfill an acceptable performance. Finally, the position and velocity estimation errors have been presented in Figs. 5 and 6, respectively. To show the important role of the proposed observer–controller in fulfilling an efficient tracking performance, the simulation is repeated by neglecting $\hat{\eta}(t)$ in (12). This condition is indeed the best scenario to examine the system uniformly ultimately bounded stability because the approximation error ε_η is not ignored. That is to say, the estimation error, ε_η has its maximum value in this scenario. Figure 7 illustrates the path tracking performance regarding this condition. According to the results, the proposed controller–observer structure can fulfill a good trajectory performance in the existence of uncertainties and external results. The performances

https://doi.org/10.1017/S0263574721001120 Published online by Cambridge University Press

Table I. *A comparison among the proposed method, RBFNN, and the fuzzy approach.*

	Requiring to state feedback or their estimated values for function approximation	**Adjustable approximator parameters**	**Implementation**
Proposed approach	No	Γ_η	Simple
RBFNN	Yes	Γ_η, c_i, $\delta_i$for i = 1,. . .,N1	Hard
Fuzzy system	Yes	Γ_η, $\hat{y}_l$, σ	Hard

of the proposed Bernstein–Stancu and the RBFNN approximators are nearly the same due to the universal approximation characteristic of these methods. However, there are more adjustable parameters in the regressor vector of the RBFNN (such as the width and center of the Gaussian units), and assigning the best values for these parameters is tedious and time-consuming due to the repeated trial and error. Furthermore, unlike neural network/fuzzy methods, which require system states as inputs to estimate functions and construct a regressor vector, the proposed Bernstein–Stancu-based approach is not dependent on the system states. The reason is that these approximators consider the uncertainty as a time-varying function rather than a function of different system states. Besides, the number of system states, as the leading factor in determining the dimension of the basis function vectors, does not affect the Bernstein–Stancu-based adaptive control strategy. Hence, the Bernstein–Stancu-based controller as a simpler structure and less computational complexity than RBFNN. Besides, the Bernstein–Stancu estimator has a significantly better performance in comparison with the fuzzy approximator. The weakness of the fuzzy method is improvable by increasing the learning rate and the number of basis functions, although it leads to another problem called as the curse of dimensionality. Table I summarizes the merits of the introduced approach in comparison with the RBFNN and the fuzzy system.

6. Conclusion

In this article, a recent control approach is used to confront uncertainties and disturbances in robot arms. For this purpose, first, unmodeled dynamics and disturbances are aggregated as the lumped uncertainty. Then, the Bernstein–Stancu polynomial as a FAT is used due to its universal approximation property to estimate the lumped uncertainty. According to the Lyapunov theorem, adaptive rules for updating polynomial coefficients are obtained in such a way as to maintain system stability. The proposed method is regressor-free, and therefore, it does not have the problems of adaptive approaches. To the best of the authors' knowledge, the Bernstein–Stancu polynomial has not previously been used to control robotic systems. Besides, the adaptive form of the Bernstein–Stancu polynomial has not been used in the previous studies. One of the advantages of the proposed method is being model-free that makes it robust in confronting the unmodulated dynamics. It is worth noting that, in this method, there is no need to know the bounds of uncertainties. Moreover, the introduced controller–observer structure does not need velocity measurements to control the system. Also, unlike many common control approaches, in this article, the voltage signal is considered as the control signal instead of the torque, and the actuator dynamics are not neglected. To evaluate and analyze the performance of the adaptive FAT-based controller, it is applied to a 2-DOF manipulator. The results indicate the robustness of the introduced approach against unmodulated dynamics and perturbations.

References

[1] Y. Kali, M. Saad and K. Benjelloun, Optimal super-twisting algorithm with time delay estimation for robot manipulators based on feedback linearization. *Robot Auton Syst.* **108**, 87–99 (2018). https://doi.org/10.1016/j.robot.2018.07.004.

[2] F. F. Silva and B. V. Adorno, Whole-body control of a mobile manipulator using feedback linearization and dual quaternion algebra. *J Intell Robot Syst.* **91**(2), 249–262 (2018). https://doi.org/10.1007/s10846-017-0686-3.

https://doi.org/10.1017/S0263574721001120 Published online by Cambridge University Press

[3] Y. Taira, S. Sagara and M. Oya, Model-based motion control for underwater vehicle-manipulator systems with one of the three types of servo subsystems. *Artif Life Robotics.* **25**(1), 133–148 (2020). https://doi.org/10.1007/s10015-019-00564-8.
[4] A. Izadbakhsh and S. Khorashadizadeh, Single-loop PID controller design for electrical flexible-joint robots. *J Braz. Soc. Mech. Sci. Eng.* **42**, 91 (2020). https://doi.org/10.1007/s40430-020-2172-25.
[5] A. Izadbakhsh, S. Khorashadizadeh and P. Kheirkhahan, Real-time Fuzzy Fractional-order control of Electrically driven flexible-joint robots, *AUT Journal of Modeling, and Simulation*, (2018). DOI: 10.22060/MISCJ.2018.13523.5075.
[6] A. Izadbakhsh and S. Khorashadizadeh, Neural control of robot manipulators considering motor voltage saturation: performance evaluation and experimental validation, *COMPEL - The International Journal for Computation and Mathematics in Electrical and Electronic Engineering* **40**(1), 27–29 (2021). https://doi.org/10.1108/COMPEL-03-2020-0127.
[7] A. Izadbakhsh and S. Khorashadizadeh, Robust adaptive control of robot manipulators using Bernstein polynomials as universal approximator, *International Journal of Robust and Nonlinear Control* **30**, 2719–2735 (2020).
[8] X. Wang, X. Liu, L. Chen and H. Hu, Deep-learning damped least squares method for inverse kinematics of redundant robots. *Measurement* **171**, 108821 (2021). https://doi.org/10.1016/j.measurement.2020.108821.
[9] B. Xian, M. S. De Queiroz, D. M. Dawson and M. L. McIntyre, Output feedback variable structure-like control of nonlinear mechanical systems. *In 42nd IEEE Int. Conf. Decision and Control* **1**, 368–373 (2003). https://doi.org/10.1109/CDC.2003.1272589.
[10] R. Ortega, J. A. Perez, P. J. Nicklasson and H. J. Sira-Ramirez, *Passivity-based control of Euler-Lagrange systems: Mechanical, electrical and electromechanical applications*. Springer Science & Business Media; 2013. https://doi.org/10.1007/978-1-4471-3603-3.
[11] G. Antonelli, F. Caccavale, S. Chiaverini and L. Villani, Tracking control for underwater vehicle-manipulator systems with velocity estimation. *IEEE J. Ocean. Eng.* **25**(3), 399–413 (2000). https://doi.org/10.1109/48.855403.
[12] Z. Yang, J. Peng and Y. Liu, Adaptive neural network force tracking impedance control for uncertain robotic manipulator based on nonlinear velocity observer. *Neurocomputing* **331**, 263–280 (2019). https://doi.org/10.1016/j.neucom.2018.11.068.
[13] D. M. Tuan and P. D. Hieu, Adaptive Position/Force Control for Robot Manipulators Using Force and Velocity Observer. *J. Electr. Eng. Technol.* **14**(6), 2575–2582 (2019). https://doi.org/10.1007/s42835-019-00281-z.
[14] K. Shojaei, A. Kazemy and A. Chatraei, An Observer-Based Neural Adaptive PID2 Controller for Robot Manipulators Including Motor Dynamics with a Prescribed Performance. *IEEE/ASME Trans Mechatron* 2020; https://doi.org/10.1109/TMECH.2020.3028968.
[15] M. Van and S. S. Ge, Adaptive fuzzy integral sliding mode control for robust fault tolerant control of robot manipulators with disturbance observer. *IEEE Trans Fuzzy Syst.* 2020; https://doi.org/10.1109/TFUZZ.2020.2973955.
[16] Y. Shang, Consensus seeking over Markovian switching networks with time-varying delays and uncertain topologies. *Appl. Math. Comput.* **273**, 1234–1245 (2016). https://doi.org/10.1016/j.amc.2015.08.115.
[17] Y. Shang, Consensus of noisy multiagent systems with Markovian switching topologies and time-varying delays. *Math. Probl. Eng.* **2015**, 1–13 (2015). https://doi.org/10.1155/2015/453072.
[18] Y. Hu, S. Dian, R. Guo, S. Li and T. Zhao, Observer-based dynamic surface control for flexible-joint manipulator system with input saturation and unknown disturbance using type-2 fuzzy neural network. *Neurocomputing* **436**, 162–173 (2021). https://doi.org/10.1016/j.neucom.2020.12.121.
[19] Y. Wu, R. Huang, X. Li and S. Liu, Adaptive neural network control of uncertain robotic manipulators with external disturbance and time-varying output constraints. *Neurocomputing* **323**, 108–116 (2019). https://doi.org/10.1016/j.neucom.2018.09.072.
[20] A. Izadbakhsh and P. Kheirkhahan, An alternative stability proof for "Adaptive Type-2 fuzzy estimation of uncertainties in the control of electrically flexible-joint robots", *Journal of Vibration and Control* **25**(5), 977–983 (2019).
[21] S. Haonan, S. Xingling and Z. Wendong, Fuzzy rule-based neural appointed-time control for uncertain nonlinear systems with aperiodic samplings. *Expert Syst Appl.* **170**, 114504 (2021). https://doi.org/10.1016/j.eswa.2020.114504.
[22] A. Izadbakhsh, Robust adaptive control of voltage saturated flexible joint robots with experimental evaluations, *AUT Journal of Modeling, and Simulation* **50**(1), 31–38 (2018).
[23] P. Kheirkhahan and A. Izadbakhsh, Observer-based adaptive fractional-order control of flexible-joint robots using the Fourier series expansion: theory and experiment. *J Braz Soc Mech Sci Eng.* **42**(10), 1–0 (2020). https://doi.org/10.1007/s40430-020-02590-1.
[24] A. Izadbakhsh, P. Kheirkhahan and S. Khorashadizadeh, FAT-based robust adaptive control of electrically driven robots in interaction with environment, *Robotica* **37**(5), 779–800 (2019). 12.
[25] A. Izadbakhsh, S. Khorashadizadeh and P. Kheirkhahan Tracking control of electrically driven robots using a model free observer. *Robotica* **37**(4), 729–755 (2019).
[26] A. Izadbakhsh and S. Khorashadizadeh, Robust task-space control of robot manipulators using differential equations for uncertainty estimation. *Robotica* **35**(9), 1923 (2017). https://doi.org/10.1017/S0263574716000588.
[27] A. Izadbakhsh, A. Akbarzadeh kalat and S. Khorashadizadeh, (2021) Observer-based adaptive control for HIV infection therapy using the Baskakov operator, *Biomedical Signal Processing and Control*, **65**.
[28] A. Izadbakhsh, FAT-based robust adaptive control of electrically driven robots without velocity measurements. *Nonlinear Dynamics.* **89**(1), 289–304 (2017). https://doi.org/10.1007/s11071-017-3454-9.
[29] D. D. Stancu, Approximation of functions by a new class of linear polynomial operators. *Rev. Roumaine Math. Pures Appl.* **13**(8), 1173–1194 (1968).

https://doi.org/10.1017/S0263574721001120 Published online by Cambridge University Press

[30] A. Izadbakhsh and S. Khorashadizadeh, Polynomial-Based Robust Adaptive Impedance Control of Electrically Driven Robots. *Robotica*, 1–21 (2020). doi: 10.1017/S0263574720001009.
[31] D. M. Dawson, Z. Qu and J. J. Carroll, Tracking control of rigid-link electrically–driven robot manipulators. *Int J Control.* **56**(5), 991–1006 (1992). https://doi.org/10.1080/00207179208934354.
[32] Y. Shang, Fixed-time group consensus for multi-agent systems with non-linear dynamics and uncertainties. *IET Control Theory Appl.* **12**(3), 395–404 (2018). https://doi.org/10.1049/iet-cta.2017.1021.
[33] A. Izadbakhsh and S. M. R. Rafiei, Endpoint perfect tracking control of robots – A robust non inversion-based approach, *International Journal of Control, Automation, and Systems*, Springer, **7**(6), 888–898 (2009).
[34] A. Izadbakhsh S. Khorashadizadeh and S. Ghandali, Robust Adaptive Impedance Control of Robot Manipulators Using Szasz-Mirakyan Operator as universal Approximator, *ISA Transactions* **106**, 1–11 (2020).

Cite this article: A. Izadbakhsh and N. Nikdel (2022). "Robust adaptive controller–observer scheme for robot manipulators: a Bernstein–Stancu approach", Robotica **40**, 1309–1325. https://doi.org/10.1017/S0263574721001120
https://doi.org/10.1017/S0263574721001120 Published online by Cambridge University Press